Three-Dimensional Structure of Thin Myocardial Filaments in Cardiac Insufficiency Caused by Toxic Allergic Myocarditis

T. G. Samsonidze, D. D. Eristavi, and N. V. Karsanov

Translated from *Byulleten' Eksperimental'noi Biologii i Meditsiny*, Vol. 127, No. 1, pp. 101-105, January, 1999
Original article submitted August 17, 1998

Diffraction patterns of a single myocardial thin filament and its Mg-paracrystals from normal myocardium and in cardiac insufficiency caused by toxic allergic myocarditis were presented, and three-dimensional reconstruction of normal and pathological filaments was carried out. It was shown that in a rigor solution pathological actin protomers are elongated, while normal filaments are kidney-shaped. It is concluded that changes in the thin myocardial filament helix parameters in heart failure caused by toxic allergic myocarditis are due to the loss of conformational mobility of native actin filaments.

Key Words: *structure; three-dimensional reconstruction; thin myocardial filaments; heart failure*

Actin plays an essential role in the development of the force of muscular contraction. Its structural abnormalities in cardiac insufficiency (CI) lead to impaired contractility of myocardial proteins [5,6]. The aim of the present study was three-dimensional reconstruction of native thin myocardial filament (TMF) in severe CI induced by 3-day toxic allergic myocarditis (TAM).

MATERIALS AND METHODS

The study was carried out on native TMF obtained from 14 healthy rabbits and 15 rabbits with TAM-induced CI [1].

Native TMF consisting of actin, tropomyosin, and troponin were isolated as described previously [7,9]. Triton X-100 in a concentration of 0.5% was used only for isolation of skien fibers. Ionic strength of all solutions was about 0.1 M. Isolated TMF were dissolved in 10 mM acetate (not phosphate) buffer containing 0.1 M KCl, 2 mM $MgCl_2$, 1 mM dithiothreitol (pH 7.0, pCa 5.5, rigor solution). Proteins were analyzed by electrophoresis in 11% polyacrylamide gel with in sodium dodecyl sulfate. Electron microphotographs of TMF (×50,000) negatively stained with 2% uranyl acetate on thin carbonic films were studied in a JEM-100B microscope (JEOL) operated at 80 kV. Negatives of solitary TMF for computer reconstruction were selected using an optic diffractometer and an IBAS 2000 image analysis system (Kontron Electronics Group) from regular undistorted fragment. High resolution in three-dimensional reconstruction was attained by analyzing the microphotographs in a PDS 1010A microdensitometer (Perkin Elmer). The data were processed using the method of projection-modifying functions [2,3]. The models were constructed from 5-mm-thick plastic plates corresponding to 9.2Å protein structure (the software created by Dr. E. V. Orlova, Institute of Crystallography, Russian Academy of Sciences).

Magnesium paracrystals were prepared by dialyzing TMF solution against 10 mM sodium acetate buffer (pH 7.0) containing 20 mM $MgCl_2$ for 48 h. Eight or 5 diffraction patterns were analyzed for normal and pathological TMF, respectively.

Republican Center for Medical Biophysics, Health Ministry, Tbilisi, Georgia

0007-4888/99/0001-0091 $22.00

RESULTS

The diameter (Δ) of native TMF in the rigor solution measured directly and calculated from diffraction patterns was about 95Å (80-100Å) in the control and about 130Å in TAM-induced CI (120-140Å). These differences were also present on optic diffraction pictures obtained after elimination of weak accidental reflections.

Period (*c*) of native TMF in the rigor solution in the control varied from 720 to 800Å due to instability of the transfer constant (at a constant elementary angle). In CI, the period of TMF extended from 570 to 1100Å despite marked narrowing of the transfer constant range.

In the control, meridional reflection on the 28th layer line corresponding to transfer constant of 27.5Å (the distance between contralateral TMF protomer projections on the helix axis) is multiply split, which reflects the transfer constant variation within 24.5-30.5Å (with a discrete period of 1Å (Fig. 2, *a*) [4,8]). In CI (Fig. 2, *b, c*), meridional reflections are shifted to the 25th and 21st layer lines, while the range of transfer constant considerably narrows to 26.5-28.5Å (also with a 1Å period).

Thus, the most prominent feature of the TMF diffraction pattern in TAM (Fig. 2, *c, d*) is a considerable shift of all layer line intensities to the meridian resulting in a 1.4-fold closer distances between parameridional reflections in comparison with the control. This attests to a proportional increase in the ΔTMF in TAM, thus confirming visual observations and direct measurements of TMF diameter on microphotographs. The increase in ΔTMF in CI is due to straightening of actin protomer and linear elongation of its external domain, as demonstrated by the disappearance of forbidden reflection corresponding to 55Å periodicity

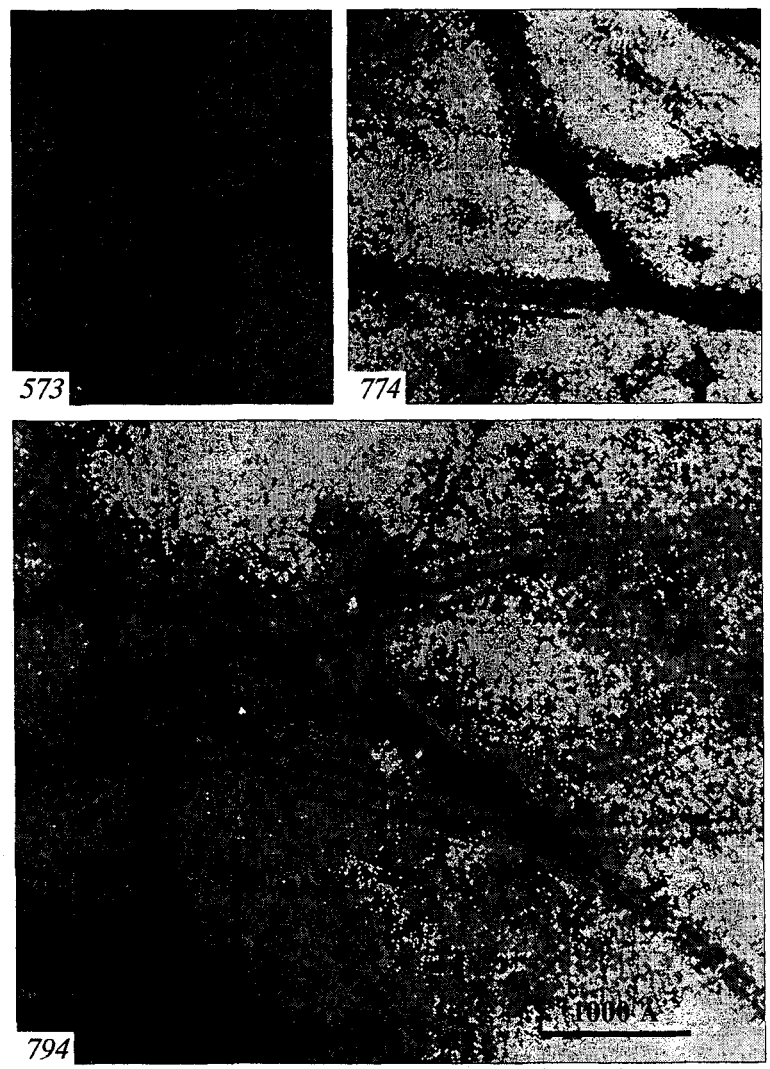

Fig. 1. Microphotographs of solitary native thin myocardial filaments from normal rabbit (*573*) and from rabbit with toxic allergic myocarditis (*794*) and of Mg-paracrystals (*774*). Solid lines indicate filament fragments containing 1-2 periods used in the analysis, ×200,000.

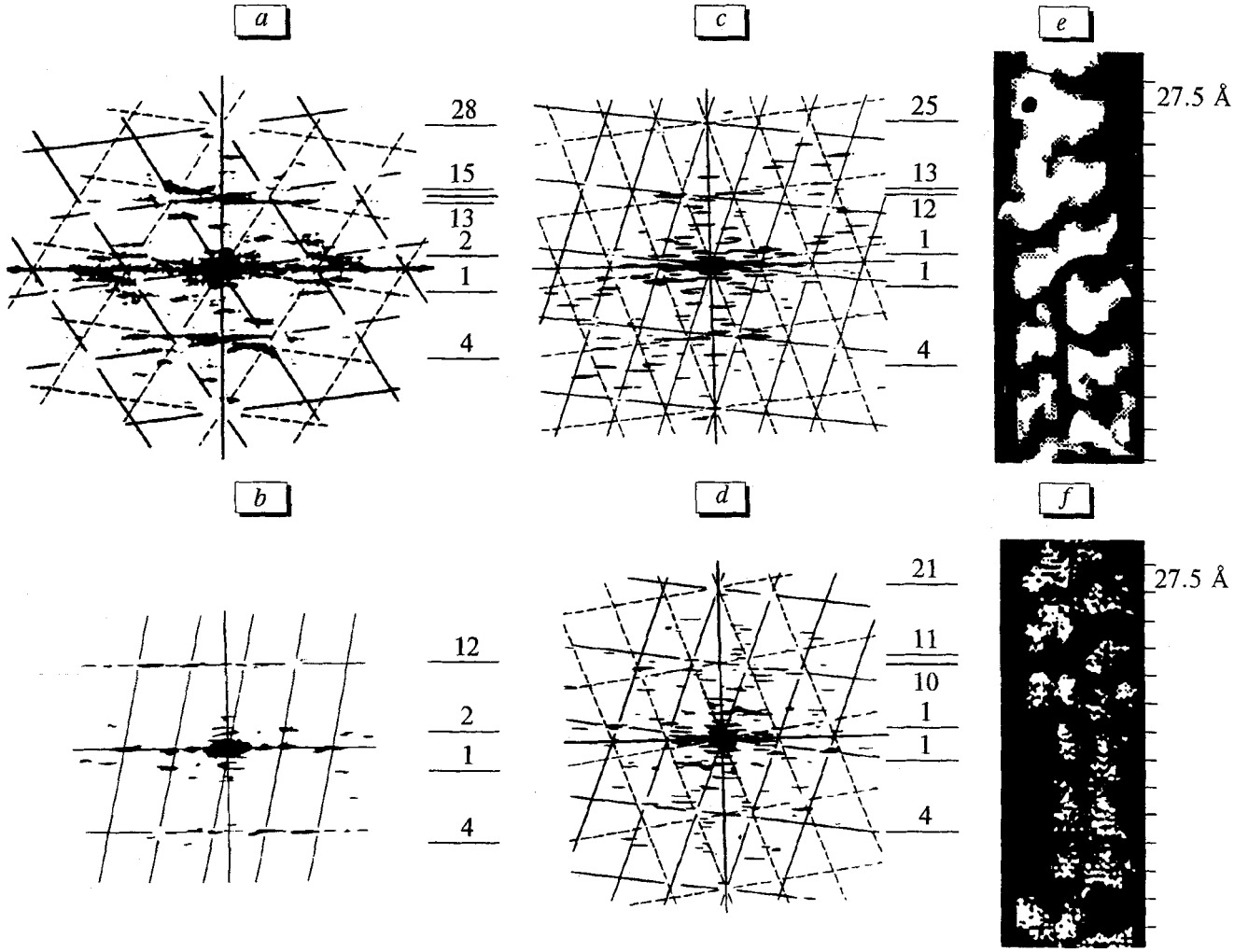

Fig. 2. Computer diffraction patterns of native thin myocardial filaments from normal rabbit (*a*) and from rabbit with toxic allergic myocarditis (*c*, *d*), and of Mg-paracrystals (*b*). Reflections from the front and back helix surfaces lie in the lattice sites indicated by solid and dotted lines, respectively. Layer lines of the major (actin) and additional (tropomyosin) periodicities are indicated above and below the equator, respectively. *e*, *f*: fragments of thin myocardial filaments indicated on microphotograph *794* (*1* and *2*, respectively) after background was subtracted. Transfer constant in 27.5Å along the whole structure length, actin structure is extended perpendicularly to the helix axis.

(seen also on F-actin diffraction pictures from normal myocardium [4]). We attribute this reflection to an artifact of uranyl acetate staining resulting from accumulation and electron beam-induced coagulation of the dye in a groove between domains of the kidney-shaped protomer (smoothening and disappearance of the groove).

In TAM-induced CI, parameridional reflections normally occurring on the 13th layer line give place to reflections corresponding to 57-59-Å periodicity on the 10th (Fig. 2, *c*) and 12th (Fig. 2, *d*) layer lines which become weak and disappear, while strong reflections on the 13th (Fig. 2, *c*) or 11th (Fig. 2, *d*) layer lines corresponding to 52-53-Å periodicity are still present. Meridional reflections occur in the 25th and 21st layer lines (Fig. 2, *c*, *d*), helix periods being 687 and 577Å, respectively. Direct measurements give the same values.

The ratio between the number of protomers (p) and turns (q) in a helix period reflects the degree of helix twisting (helix twist angle $\alpha=2\pi q/p$). In TAM, q/p is equal to 25/12 (Fig. 2, *c*) or 21/10 (Fig. 2, *d*) *vs.* 28/13 in the control (Fig. 2, *a*) suggesting 171-172° twisting angle in TAM *vs.* 167° in the control.

Since c, p, and q vary considerably in the control and TAM rabbits, three-dimensional reconstruction was carried out for TMF fragments with c=687Å, p=25, and q=12, 172° twisting angle, and 27.5Å elementary disc thickness (as in the norm) to exclude the effects of various destabilizing factors. These parameters were similar to those in Mg-paracrystals and stabilized TMF.

Under these conditions the reflections from tropomyosin in the control and TAM occur in the same position. Analysis of numerous TMF diffraction pic-

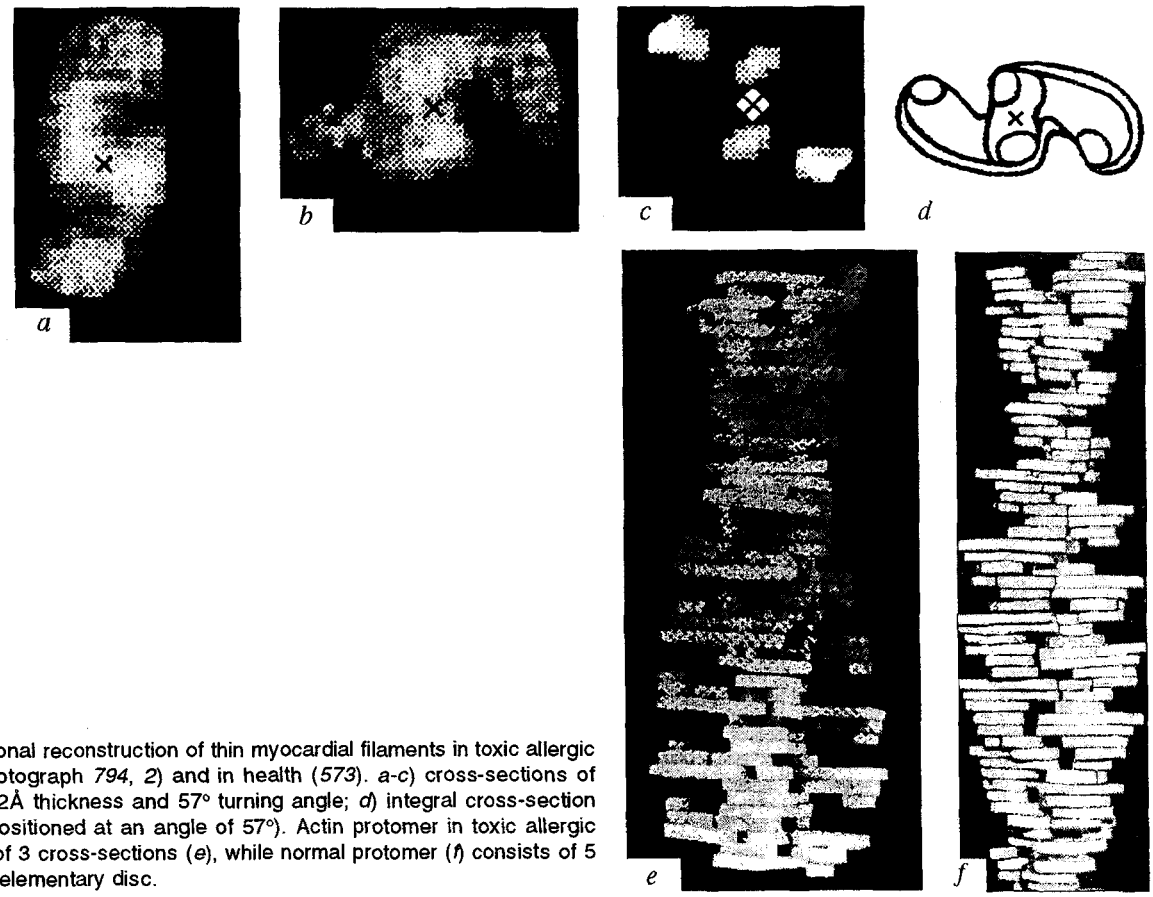

Fig. 3. Three-dimensional reconstruction of thin myocardial filaments in toxic allergic myocarditis (microphotograph *794*, *2*) and in health (*573*). *a-c*) cross-sections of elementary disc of 9.2Å thickness and 57° turning angle; *d*) integral cross-section (cross-sections *a-c* positioned at an angle of 57°). Actin protomer in toxic allergic myocarditis consists of 3 cross-sections (*e*), while normal protomer (*f*) consists of 5 cross-sections of the elementary disc.

tures shows that in both control and TAM animals 30% tropomyosin is arranged at a distance of 29Å from the helix axis. The tropomyosin reflection is liable. Two tropomyosin chains form a right-handed two-start helix with parameters c=140Å, p=2, and q=1.

Crystallization of both control and pathological TMF (Mg-paracrystals) stabilizes the structure with a fixed helix period of 770Å, despite the differences between actin structure in the norm and TAM. In TAM, the diffraction patterns of TMF-Mg (Fig. 2, *b*) paracrystals exhibits reflections on the 2nd and 12th layer lines (as in the control). Hence, the helix period in the paracrystals is stable in both cases and equal to 770Å.

As seen from computer-filtered images of TMF (Fig. 2, *e*, *f*; fragments *1* and *2* on microphotograph 794, Fig. 1), pathological actin protomer is extended perpendicularly to the helix axis attaining 90Å length, which increases ΔTMF.

Three-dimensional reconstruction TMF (Fig. 3) in TAM shows three cross-sections of elementary discs crossing 2 contralateral protomers. Each disc is characterized by thickness ($\Delta=c/p$) $\Delta'=\Delta/3=27.5/3=9.2$Å and twisting angle $\alpha'=\alpha/3=172°/3=57°$. Superposition of these 3 cross-sections under corresponding angles yields elementary disk (Fig. 3, *d*) and constructed TMF models in the norm (Fig. 3, *f*) and TAM (Fig. 3, *e*).

Reconstructed TMF in TAM is characterized by 140Å diameter and 687Å period, the size of actin protomer is 90×40×30Å (*vs.* 65×40×45 in the norm), it folds in a right-handed helix with 27.5Å transfer constant and p/q =25/12. The slope of the external domain with the helix axis is 70° in both the norm and TAM. Tropomyosin chains are arranged at a distance of 30A from the helix axis. Compared with normal, TMF in TAM is characterized by radial elongation of actin protomers resulting in an increase in ΔTMF (Fig. 3). A wider range of the helix period values and stable transfer constant probably reflect deformation of actin protomers, and, consequently, changes in p, q, and the degree of the helix twisting. It cannot be excluded that considerable variability of helix period as well as instability of the transfer constant play a functional role and result from weakening of the protomer-protomer bonds. Thus, linear extension of the external actin domain in TAM-induced CI is associated with weakening of the bonds between domains, while the increase in helix period is associated with weakening of bonds between TMF protomers along genetic sequence,

which agrees with experimental data obtained in non-thyroid cardiomyopathy.

Our experiments show that native TMF has a labile structure. The relative stability of the normal TMF helix parameters (except for the transfer constant) due to the stabilizing effect of troponin-tropomyosin complex suggest that actin protomers play an important role in the generation of muscular strength. Indeed, variability of the transfer constant indicating the lability of protomer structure decreases considerably. Heart contractility in TAM decreases. It can be hypothesized that these conformational changes in contracting muscles are possible due to liable TMF structure, while in CI, the lability of protomer and of the entire molecule is decreased. The increase in ΔTMF and stabilization of the transfer constant (27.5Å for CI) are associated with the loss of conformational mobility. These findings substantiate the data on reduced conformational mobility of the tertiary actin structure in CI obtained by the method of circular dichroism [6].

REFERENCES

1. S. V. Andreev and M. V. Sokolov, in: *Role of Hypoxia in Pathogenesis of Toxic Myocarditis* [in Russian], Moscow (1968), pp. 91-92.
2. B. K. Vainshtein, *Kristallografiya*, **15**, 894-902 (1970).
3. B. K. Vainshtein and S. S. Orlov, *Ibid.*, **17**, 253-257 (1972).
4. N. V. Karsanov and T. G. Samsonidze, *Biofizika*, **31**, 7-9 (1986).
5. N. V. Karsanov, D. D. Eristavi, and B. G. Dzhinchvelashvili, *Izv. Akad. Nauk GSSR*, **7**, 561-568 (1981).
6. N. V. Karsanov, D. D. Eristavi, and B. G. Dzhinchvelashvili, *Ibid.*, **14**, 134-142 (1988).
7. S. Driska and D. J. Hartshorne, *Arch. Biochem. Biophys.*, **167**, No. 2, 203-212 (1975).
8. K. S. Holmes, D. Popp, W. Gebhard, and W. Kabsch, *Nature*, **347**, No. 6288, 44-49 (1990).
9. T. Obinata, I. Hayashi, and D. Fishman, *Dev. Growth Differ.*, **16**, No. 2, 105-121 (1974).
10. T. G. Samsonidze, O. N. Zograf, D. G. Khachidze, *et al.*, *J. Mol. Cell. Cardiol.*, **21**, 80 (1989).